

Synthesis, Structural Characterization, and MO Calculations of Vanadium Imido Complexes Containing Bidentate Phosphine Coligands

Francisco Montilla,[†] Angeles Monge,[‡] Enrique Gutiérrez-Puebla,[‡] Antonio Pastor,[†] Diego del Río,[†] Norge Cruz Hernández,[§] Javier Fernández Sanz,^{*,§} and Agustín Galindo^{*,†}

Departamento de Química Inorgánica, Universidad de Sevilla, Apto 553, 41071 Sevilla, Spain, Departamento de Química Física, Universidad de Sevilla, 41071 Sevilla, Spain, and Instituto de Ciencia de Materiales, CSIC, Campus de Cantoblanco, 28049 Madrid, Spain

Received January 6, 1999

Treatment of complex $V(N-2,6\text{-}i\text{Pr}_2\text{C}_6\text{H}_3)\text{Cl}_3$ with 1,2-dimethoxyethane (dme) gives in quasi-quantitative yield the adduct $V(N-2,6\text{-}i\text{Pr}_2\text{C}_6\text{H}_3)\text{Cl}_3(\text{dme})$ (**1**). Interaction of **1** with bidentate phosphines gives $V(N-2,6\text{-}i\text{Pr}_2\text{C}_6\text{H}_3)\text{Cl}_3(\text{P-P})$ (P-P = depe, **2a**; dppe, **2b**) compounds. An X-ray analysis (monoclinic, space group $P2_1/c$, $a = 14.7387$ (14) Å, $b = 10.6738$ (10) Å, $c = 16.999$ (3) Å, $\beta = 90.954$ (2)°, $Z = 4$, $R = 0.0544$), carried out on complex **2a**, shows a *mer* arrangement of the chloride ligands and a nonsymmetrical coordination of the diphosphine ligand. One of the phosphorus atoms occupies the trans position with respect to the organoimido ligand. MO calculations on the models $V(\text{NR})\text{Cl}_3(\text{H}_2\text{PCH}_2\text{CH}_2\text{PH}_2)$ ($R = \text{H}, \text{C}_6\text{H}_5$) of complex **2a** were performed. The *mer* isomer, which is more stable than the *fac* isomer, shows good agreement with the experimental data.

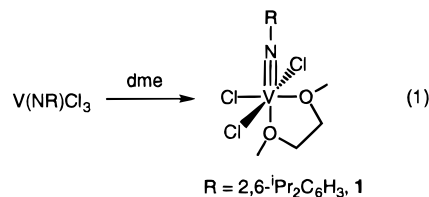
Introduction

Low metal electronic configurations are characteristic of organoimido complexes.^{1,2} On the other hand, early transition metal species in the highest formal oxidation state containing coordinated phosphine ligands are uncommon.³ Consequently, the number of characterized d^0 imido-phosphine derivatives is quite scarce.

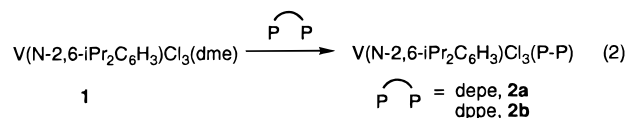
As a continuation of our work on molybdenum imido complexes,^{4,5} we decided to explore the chemical reactivity of d^0 vanadium imido compounds versus tertiary phosphines. In this paper, the preparation of vanadium imido complexes containing bidentate phosphine coligands $V(N-2,6\text{-}i\text{Pr}_2\text{C}_6\text{H}_3)\text{Cl}_3(\text{P-P})$ (P-P = depe, **2a**; dppe, **2b**) and the structural characterization of **2a** are reported. As far as we know, this is the first group 5 imido complex containing a phosphine functionality occupying the trans position with respect to the organoimido ligand. Because of the novelty of this compound, a theoretical analysis of its molecular properties based on density functional theory (DFT) calculations is also reported. The *mer* isomer of the models $V(\text{NR})\text{Cl}_3(\text{H}_2\text{PCH}_2\text{CH}_2\text{PH}_2)$ ($R = \text{H}, \text{C}_6\text{H}_5$), which is more stable than the *fac* isomer, shows good agreement with the experimental data.

Results and Discussion

Synthesis and Characterization. Crystal and Molecular Structure of 2a. Addition of 1,2-dimethoxyethane (dme) to petroleum ether solutions of the $V(N-2,6\text{-}i\text{Pr}_2\text{C}_6\text{H}_3)\text{Cl}_3$ compound^{6–8} causes precipitation in an almost quantitative yield of $V(N-2,6\text{-}i\text{Pr}_2\text{C}_6\text{H}_3)\text{Cl}_3(\text{dme})$ (**1**) as a brown solid (eq 1). NMR



spectra of **1** are in agreement with this structure and compare well with the NMR data of $\text{Ta}(\text{NR})\text{Cl}_3(\text{dme})$ ($R = 2,6\text{-}i\text{Pr}_2\text{C}_6\text{H}_3$,⁹ 1-adamantyl¹⁰) compounds. The structure proposed (eq 1) is similar to that recently reported for the analogous $V(\text{N}^i\text{Bu})\text{Cl}_3(\text{dme})$ ¹¹ and $\text{Nb}(\text{N}^i\text{Bu})\text{Cl}_3(\text{dme})$ ¹⁰ derivatives. Addition of bidentate phosphines to THF solutions of **1** produces $V(N-2,6\text{-}i\text{Pr}_2\text{C}_6\text{H}_3)\text{Cl}_3(\text{P-P})$ complexes **2a** and **2b** (eq 2).



A closely related compound $V(N-4\text{-MeC}_6\text{H}_4)\text{Cl}_3(\text{PPh}_3)$, containing only one coordinated phosphine, was reported by Maatta.⁸ Complex **2b** was obtained in good yields (70%) as an

* E-mail: galindo@cica.es and sanz@cica.es.

[†] Departamento de Química Inorgánica, Universidad de Sevilla.

[‡] X-ray study, CSIC, Madrid.

[§] Departamento de Química Física, Universidad de Sevilla.

(1) Wigley, D. E. *Prog. Inorg. Chem.* **1994**, *42*, 239.

(2) Nugent, W. A.; Mayer, J. M. *Metal-Ligand Multiple Bonds*; Wiley-Interscience: New York, 1988.

(3) McAuliffe, C. A.; Levason, W. *Phosphine, Arsine and Stibine Complexes of Transition Elements*; Elsevier: Amsterdam, 1979.

(4) Galindo, A.; Montilla, F.; Pastor, A.; Carmona, E.; Gutiérrez-Puebla, E.; Monge, A.; Ruiz, C. *Inorg. Chem.* **1997**, *36*, 2379.

(5) Montilla, F.; Galindo, A.; Carmona, E.; Gutiérrez-Puebla, E.; Monge, A. *J. Chem. Soc., Dalton Trans.* **1998**, 1299.

(6) Scheuer, S.; Fischer, J.; Kress, J. *Organometallics* **1995**, *14*, 2627.

(7) Buijink, J.-K. F.; Teuben, J. H.; Kooijman, H.; Spek, A. L. *Organometallics* **1994**, *13*, 2922.

(8) Devore, D. D.; Lichtenhan, J. D.; Takusagawa, F.; Maatta, E. A. *J. Am. Chem. Soc.* **1987**, *109*, 7408.

(9) Chao, Y.-W.; Wexler, P. A.; Wigley, D. E. *Inorg. Chem.* **1989**, *28*, 3860.

(10) Korolev, A. V.; Rheingold, A. L.; Williams, D. S. *Inorg. Chem.* **1997**, *36*, 2647.

(11) Preuss, F.; Hornung, G.; Frank, W.; Reib, G.; Müller-Becker, S. Z. *Anorg. Allg. Chem.* **1995**, *621*, 1663.

orange solid by precipitation. However, the yields of crystalline **2a** are low. This fact is probably due to a simultaneous reduction–hydrolysis process that occurs during the reaction and the subsequent workup. The isolation of the $\text{VOCl}_2(\text{depe})$ complex during the crystallization of **2a** confirms this assumption. Similar reduction–hydrolysis processes have been noticed by Cotton and co-workers in the reaction of VCl_4 with phosphines.^{12,13} **2a** and **2b** are unstable in the presence of small quantities of air, or prolonged reaction times also decrease the yields.

Both compounds exhibit two broad resonances (caused by unresolved coupling to the vanadium nucleus, $I = 7/2$, and quadrupolar effects) in the $^{31}\text{P}\{^1\text{H}\}$ NMR spectra, which is characteristic of an AX spin system (for example, δ 14.4 and 48.3, data for **2a**). Their ^1H and $^{13}\text{C}\{^1\text{H}\}$ NMR spectra are nevertheless quite informative with respect to the structure they exhibit in solution. For example, the C_s symmetry of the molecules of **2a** is manifested by the observation of two different signals for the methyl groups of the depe ligand in either spectrum. The presence of two resonances for the methylene carbon atoms of the phosphine chain in the $^{13}\text{C}\{^1\text{H}\}$ NMR spectra of both complexes definitively supports structure **I** for compounds **2**.

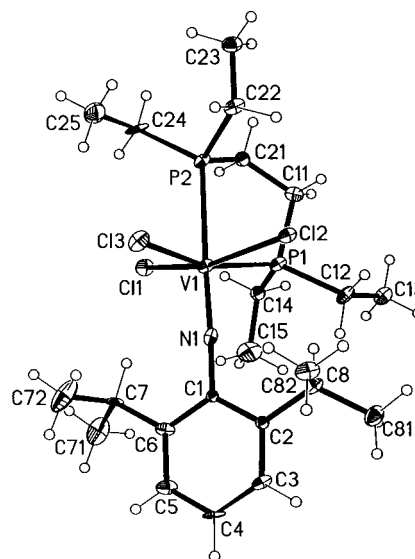
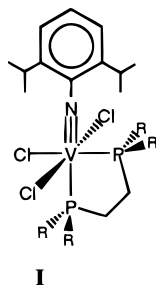


Figure 1. Molecular structure of $\text{V}(\text{N}-2,6\text{-}i\text{-Pr}_2\text{C}_6\text{H}_3)\text{Cl}_3(\text{depe})$ (**2a**).

Table 1. Selected Bond Lengths (Å) and Angles (deg) for **2a**

| | | | |
|------------------|------------|------------------|------------|
| V(1)–N(1) | 1.685(4) | V(1)–Cl(3) | 2.301(2) |
| V(1)–Cl(1) | 2.3204(14) | V(1)–Cl(2) | 2.3217(14) |
| V(1)–P(1) | 2.520(2) | V(1)–P(2) | 2.642(2) |
| N(1)–C(1) | 1.388(6) | | |
| N(1)–V(1)–Cl(3) | 99.7(2) | N(1)–V(1)–Cl(1) | 98.59(13) |
| Cl(3)–V(1)–Cl(1) | 97.96(6) | N(1)–V(1)–Cl(2) | 99.41(13) |
| Cl(3)–V(1)–Cl(2) | 93.66(6) | Cl(1)–V(1)–Cl(2) | 156.57(7) |
| N(1)–V(1)–P(1) | 95.2(2) | Cl(3)–V(1)–P(1) | 164.41(7) |
| Cl(1)–V(1)–P(1) | 84.13(5) | Cl(2)–V(1)–P(1) | 79.42(5) |
| N(1)–V(1)–P(2) | 173.6(2) | Cl(3)–V(1)–P(2) | 86.25(6) |
| Cl(1)–V(1)–P(2) | 78.31(5) | Cl(2)–V(1)–P(2) | 82.24(5) |
| P(1)–V(1)–P(2) | 79.02(5) | C(1)–N(1)–V(1) | 177.0(4) |

This geometrical disposition is peculiar because a phosphorus atom occupies the trans position with respect to the aryimido ligand. To our knowledge, only five examples of compounds with a coordinated phosphine trans with respect to an organoimido ligand have been structurally characterized for group 6. Four of them are tungsten complexes, namely, $\text{W}(\text{N}-2,6\text{-}i\text{-Pr}_2\text{C}_6\text{H}_3)\text{Cl}_3(\text{dppe})$,¹⁴ $\text{W}(\text{NPh})(\text{C}\equiv\text{CPh})_2(\text{PhC}\equiv\text{CPh})(\text{PMe}_3)_2$ ¹⁵ (Nielson and co-workers), and $\text{W}(\text{NPh})(\text{R})_2[(\text{Me}_3\text{SiN})_2\text{C}_6\text{H}_4](\text{PMe}_3)$ ($\text{R} = \text{Cl}, \text{Me}$) (Boncella and co-workers¹⁶). The other one, recently reported by us,⁴ is the somewhat related complex $\text{Mo}(\text{N}-2,4,6\text{-Me}_3\text{C}_6\text{H}_2)\text{Cl}_3(\text{depe})$. Therefore, the crystalline depe derivative **2a** was considered a suitable candidate for a solid state structural determination.

The X-ray analysis reveals a pseudooctahedral geometry with a meridional arrangement of the chloride ligands (Figure 1, Table 1).

The main distortion from the octahedral geometry comes from the typical² deviations of the $\text{N1}-\text{V1}-\text{P1}$ angle ($95.2(2)^\circ$) and the three $\text{N1}-\text{V1}-\text{Cl}$ angles ($98.59(13)^\circ$, $99.41(13)^\circ$, and $99.7(2)^\circ$) from the ideal 90° value. The metal–imido moiety is practically linear ($177.0(4)^\circ$, $\text{V1}-\text{N1}-\text{C1}$), and the $\text{V1}-\text{N1}$ separation of $1.685(4)$ Å is in agreement with a vanadium–nitrogen bond order of 3. The bidentate depe ligand is

nonsymmetrically coordinated to the metal atom with a normal $\text{V1}-\text{P1}$ distance of $2.520(2)$ Å and an unusually large $\text{V1}-\text{P2}$ bond length of $2.642(2)$ Å. Structurally characterized vanadium–depe complexes display vanadium–phosphorus bond distances in the range $2.50\text{--}2.57$ Å;^{17–19} meanwhile vanadium–phosphorus bond lengths usually cluster around the mean $2.482(5)$ Å value.²⁰ Accordingly, the $\text{V1}-\text{P2}$ separation of $2.642(2)$ Å in **2a** can be considered as remarkably large and can be interpreted in terms of the strong trans influence of the imido ligand. Longer $\text{V}-\text{P}$ bond distances ($2.817(3)$ and $2.826(3)$ Å) have been reported²¹ only in the case of complex $\{[(\text{Ph}_2\text{P})_2\text{CH}_3\text{V}]\text{[Li}(\text{THF})_4](\text{THF})_2\}$ and were attributed to crystal packing effects. A similar $\text{V}-\text{P}$ bond distance is encountered in $\text{VOCl}_2(\text{PPh}_3)_2$ ($2.6217(11)$ Å),¹² and lower bond lengths were found in two other structurally characterized vanadium(V) imido–phosphine complexes ($2.4010(19)$ Å in $\text{CpV}(\text{N}-2,6\text{-}i\text{-Pr}_2\text{C}_6\text{H}_3)(\text{CHPh})(\text{PMe}_3)$ ⁷ and $2.529(1)$ Å in $\text{V}(\text{NPM}_2\text{Ph})\text{Cl}_3(\text{PMe}_2\text{Ph})_2$).²²

(12) Cotton, F. A.; Lu, J. *Inorg. Chem.* **1995**, *34*, 2639.

(13) Cotton, F. A.; Lu, J.; Ren, T. *Inorg. Chim. Acta* **1994**, *215*, 47.

(14) Clark, G. R.; Glenney, M. W.; Nielson, A. J.; Rickard, C. E. *J. Chem. Soc., Dalton Trans.* **1995**, 1147.

(15) Clark, G. R.; Nielson, A. J.; Rickard, C. E. *J. Chem. Soc., Chem. Commun.* **1989**, 1157.

(16) Boncella, J. M.; Wang, S.-Y. S.; VanderLende, D. D.; Huff, R. L.; Abboud, K. A.; Vaughn, W. M. *J. Organomet. Chem.* **1997**, *530*, 59.

(17) Henderson, R. A.; Hills, A.; Hughes, D. L.; Lowe, D. J. *J. Chem. Soc., Dalton Trans.* **1991**, 1755.

(18) Holt, D. G. L.; Larkworthy, L. F.; Povey, D. C.; Smith, G. W.; Leigh, G. *J. Inorg. Chim. Acta* **1993**, *207*, 11.

(19) Hitchcock, P. B.; Hughes, D. L.; Leigh, G. J.; Sanders, J. R.; de Souza, J.; McGarry, C. J.; Larkworthy, L. F. *J. Chem. Soc., Dalton Trans.* **1994**, 3683.

(20) Cambridge Crystallographic Database search: Allen, F. H.; Davies, J. E.; Galloy, J. J.; Johnson, O.; Kennard, O.; Macrae, C. F.; Watson, D. G. *J. Chem. Inf. Comput. Sci.* **1991**, *31*, 204.

(21) Edema, J. J. H.; Meetsma, A.; van Bolhuis, F.; Gambarotta, S. *Inorg. Chem.* **1991**, *30*, 2056.

(22) Hills, A.; Hughes, D. L.; Leigh, G. J.; Prieto-Alcon, R. *J. Chem. Soc., Dalton Trans.* **1993**, 3609.

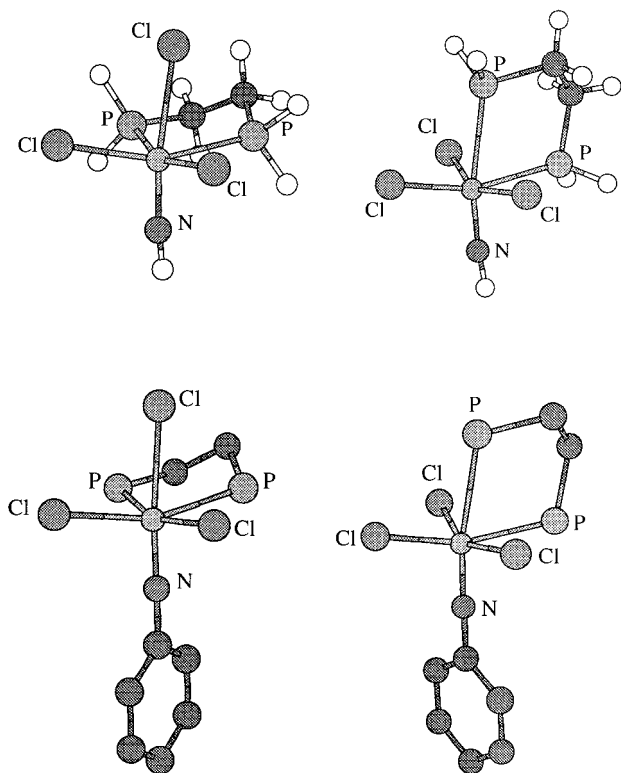


Figure 2. Final optimized geometries of *fac* and *mer* isomers of $V(NR)Cl_3(H_2PCH_2CH_2PH_2)$ ($R = H, C_6H_5$) models. For $R = C_6H_5$, hydrogen atoms are not displayed.

Examples of vanadium complexes containing other triple bonded ligands with a trans phosphine ligand are known for the carbyne functionality (for example, $V(CR)(CO)(dmpe)_2^{23}$). However, no example has been reported for an oxo derivative. Efforts are in progress to get new candidates for this geometrical disposition.

Theoretical Calculations on Model Compounds of 2a. To get a deeper insight into the structure of compound **2a** a series of model theoretical calculations were performed. Because of the high number of atoms, and with the aim to speed the calculations, the analysis was undertaken using a model in which the $(N-2,6-Pr_2C_6H_3)$ ligand was replaced by an NR group, with $R = H, C_6H_5$. Also, the depe bidentate phosphine was substituted by $(H_2PCH_2CH_2PH_2)$.

Two different arrangements were considered for this model compound and correspond to the *fac* and *mer* isomers, respectively, of parent compound **2a**. The final optimized geometries of these isomers are depicted in Figure 2, while selected structural parameters are reported in Table 2. For the sake of comparison, the experimental data are also included in the table. In general, and taking into account that the models are significantly less hindered, one can observe quite a satisfactory agreement between the *mer* and experimental values of geometrical parameters. Bond distances agree within 0.06 Å, while the largest deviation of bond angles appears to be about 6°. The structural data of Table 2 deserve a more careful analysis. Starting with the V–N bond length, it turns out that, whatever the basis set is, this distance is underestimated by 0.04 Å when $R = H$. This result suggests that such a simple model could not be suitable enough. Actually, when the NH imido ligand is replaced by NC_6H_5 , a relaxation of the V–N bond is observed, leading to a better agreement with the experimental value. V–Cl

Table 2. Selected Bond Distances (Å) and Bond Angles (deg) Obtained for *fac* and *mer* $V(NR)Cl_3(H_2PCH_2CH_2PH_2)$ Models

fac-

mer-

| | R = H | | | | R = C ₆ H ₅ | | exptl |
|---------|------------|------------|------------|------------|-----------------------------------|------------|-------|
| | basis I | | basis II | | basis I | | |
| | <i>fac</i> | <i>mer</i> | <i>fac</i> | <i>mer</i> | <i>fac</i> | <i>mer</i> | |
| V–N | 1.654 | 1.643 | 1.653 | 1.642 | 1.675 | 1.664 | 1.685 |
| V–Cl1 | 2.257 | 2.344 | 2.251 | 2.338 | 2.265 | 2.352 | 2.320 |
| V–Cl2 | 2.559 | 2.335 | 2.545 | 2.332 | 2.538 | 2.337 | 2.322 |
| V–Cl3 | 2.251 | 2.248 | 2.246 | 2.242 | 2.258 | 2.252 | 2.301 |
| V–P1 | 2.494 | 2.529 | 2.482 | 2.511 | 2.497 | 2.534 | 2.520 |
| V–P2 | 2.492 | 2.710 | 2.484 | 2.689 | 2.495 | 2.699 | 2.642 |
| P1–C1 | 1.879 | 1.875 | 1.869 | 1.866 | 1.879 | 1.876 | 1.835 |
| P2–C2 | 1.873 | 1.883 | 1.864 | 1.874 | 1.873 | 1.884 | 1.832 |
| C1–C2 | 1.554 | 1.556 | 1.537 | 1.538 | 1.555 | 1.556 | 1.541 |
| N–V–Cl1 | 101.4 | 98.8 | 101.4 | 98.8 | 98.9 | 98.0 | 98.6 |
| N–V–Cl2 | 161.4 | 98.4 | 161.7 | 98.1 | 164.7 | 98.6 | 99.4 |
| N–V–Cl3 | 100.9 | 105.3 | 101.0 | 105.8 | 98.4 | 103.0 | 99.7 |
| N–V–P1 | 91.3 | 92.6 | 90.9 | 91.8 | 92.1 | 93.3 | 95.2 |
| N–V–P2 | 93.8 | 168.3 | 93.3 | 168.0 | 96.0 | 169.5 | 173.6 |

bond distances agree noticeably with the exception of the V–Cl3 one, which is always underestimated by ca. 0.05 Å. Because of this shorter distance, repulsion between the Cl3 atom and imido group increases, leading to larger N–V–Cl3 bond angles. Notice how, disregarding the basis set used in the computations, these angles are found to be about 105° when $R = H$ and, in fact, account for the largest deviations observed in the bond angles. Moreover, it is also worth noting that, for $R = C_6H_5$, this bond angle lowers according to the drop of the repulsion induced by the lengthening of the V–N bond distance. Concerning the V–P bond lengths, the equatorial V–P1 ones are always found in quite good agreement with the experiment; however, the axial V–P2 distances appear to be systematically overestimated by 0.04–0.07 Å. The best result is obtained with basis II, although the improvement is moderate. A similar trend is observed in the P–C bond distances, on which the use of a better basis set gives rise to a moderately improved agreement. Finally, the C–C distances agree within 0.015 Å. In summary, all of these considerations suggest that the structure of this compound arises from a complex compromise between electronic and steric effects whose modeling slightly depends on the basis set and the nature of the imido group, although the use of NC_6H_5 instead of NH appears preferable.

One of the most outstanding structural aspects of compound **2a** is the large trans influence induced by the imido group. Thus, the V–P2 distance is found to be significantly stressed with respect to a normal V–P bond. In particular, the V–P interatomic distances are 2.520(2) and 2.642(2) Å for cis and trans dispositions, respectively. Such a trans influence is nicely reproduced by the theoretical calculations, which give rise to V–P distances of 2.534 and 2.699 Å. A similar trans influence is observed in the *fac* series, where the V–Cl(trans) bond distance is found to be 0.27–0.28 Å larger than the VCl(cis) one (V–Cl1 = 2.265 Å, V–Cl2 = 2.538 Å, and V–Cl3 =

(23) Protasiewicz, J. D.; Lippard, S. J. *J. Am. Chem. Soc.* **1991**, *113*, 6564.

(24) Lyne, P. D.; Mingos, D. M. P. *J. Chem. Soc., Dalton Trans.* **1995**, 1635.

(25) Lyne, P. D.; Mingos, D. M. P. *J. Organomet. Chem.* **1994**, *478*, 141.

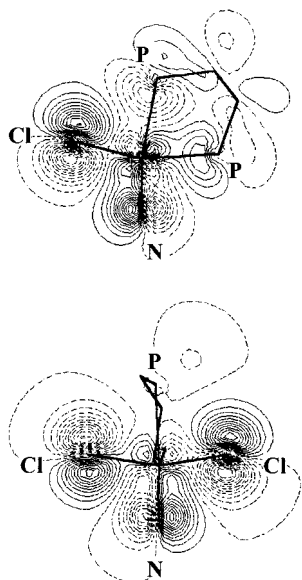


Figure 3. Contour plots for the HOMO (top) and HOMO-1 (bottom) of the model of $V(NH)Cl_3(H_2PCH_2CH_2PH_2)$, showing the two components of the π imido–V bond.

2.258 Å). The origin of the trans influence has been examined in Os nitride²⁴ and Mo imido²⁵ complexes and very recently in Ti imido²⁶ derivatives and has been mainly ascribed to electronic effects. It has been proposed that increasing the bond angles between the imido group and equatorial ligands diminishes the metal–Cl(cis) antibonding interaction, while it favors the π overlap between the metal and imido ligand. Our calculations fully support this interpretation as shown in Figure 3, where the two highest occupied molecular orbitals are depicted. These plots correspond to the orbital contours in the planes N–V–P–P (HOMO, top) and N–V–P–Cl (HOMO-1, bottom) and show two components of the formally double π N–V bond. It clearly appears that bending away the equatorial ligands allows for some V dp hybridization, increasing the overlap with N orbitals. Concomitantly, the Cl p orbitals lower the antibonding interaction with V d orbitals. However, such a bending increases the Cl–P(trans) antibonding interaction, as clearly observed in the contour plot of the HOMO, where a large contribution of P(trans) is found. This repulsive interaction is again lowered by a lengthening of the V–P(trans) bond distance. Notice on the other hand that such an “umbrella” effect is not exclusive of imido ligands, but it has been observed associated with other transition metal compounds containing multiple bonded ligands,² like carbene²⁷ and analogous derivatives.

Concerning the energetics of the system, the *mer* isomers are always found to be more stable than the *fac* models. The energy differences are computed to be 3.8 (basis I) and 3.7 kcal/mol (basis II) when R = H, while for R = C₆H₅, the stabilization of the *mer* isomer increases up to 5.4 kcal/mol. This result supports the weak dependence on the basis set and is also in agreement with the fact that only the *mer* isomer is isolated. The origin of the larger stability of *mer* isomers can be rationalized analyzing the different way in which formally d⁰ metal imido derivatives can bind a phosphine or chloride ligand. For phosphine, the main contribution to the bond is the σ donation toward the metal; however, for chloride, aside from this σ donation, there is an interaction between the filled Cl p orbitals and the metal (π

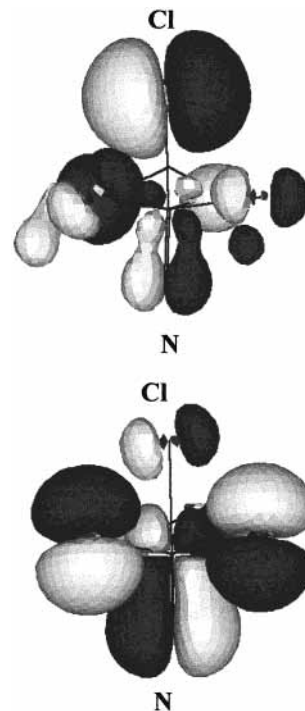


Figure 4. 3D isosurfaces corresponding to the in phase (bottom) and out of phase combinations of the 3p Cl orbital and the N–V π molecular orbital.

donation). Considering the interaction between a p Cl orbital and d V ones, say 3p_x and d_{xz} levels, it turns out that the latter is largely involved in the bond with the imido group, and in fact, the interaction takes place with the V–N π orbital. This consists of a 2-orbital/4-electron interaction which relatively destabilizes the complex. These considerations are illustrated in Figure 4, where the HOMO-3 (bottom) and HOMO-1 (top) orbitals are depicted. As observed, the mix of the 3p Cl orbital and the V–N π orbital leads to *in phase* (mainly V–N π orbital) and *out of phase* (mainly Cl 3p orbital) combinations according to the classical 2-MO/4-electron description.

Experimental Section

All preparations and other operations were carried out under a dry oxygen-free nitrogen atmosphere following conventional Schlenk techniques. Solvents were dried and degassed before use. Microanalyses were carried out by the Microanalytical Service of the University of Sevilla. Infrared spectra were recorded on a Perkin-Elmer model 883 spectrophotometer. ¹H, ¹³C, and ³¹P NMR spectra were run on Bruker AMX-300 and Bruker AMX-500 spectrometers. ³¹P shifts were measured with respect to external 85% H₃PO₄. ¹³C NMR spectra were referenced using the ¹³C resonance of the solvent as an internal standard but are reported with respect to SiMe₄. The petroleum ether used had bp 40–60 °C.

V(N-2,6-Pr₂C₆H₃)Cl₃(dme) (1). A solution of the V(N-2,6-Pr₂C₆H₃)Cl₃ complex (prepared according to the literature procedure^{6–8} from VOCl₃ (2.19 g, 12.6 mmol) and 2,6-Pr₂C₆H₃NCO (2.57 g, 12.6 mmol)) in petroleum ether (80 mL) was treated with 1,2-dimethoxyethane (10 mL). The resulting suspension was stirred for a few minutes and filtered. The collected brown solid was washed with petroleum ether and dried under vacuum (90% yield). ¹H NMR (300 MHz, C₆D₆): δ 6.87 (d, ³J_{HH} = 7.6 Hz, 2, CH meta), 6.63 (t, ³J_{HH} = 7.6 Hz, 1, CH para), 5.27 (sept, ³J_{HH} = 6.6 Hz, 2, CH(CH₃)₂), 3.32 (br s, 6, CH₃O), 3.21 (br s, 4, OCH₂), 1.41 (d, ³J_{HH} = 6.6 Hz, 12, CH(CH₃)₂). ¹³C{¹H} NMR (75 MHz, C₆D₆): δ 154.9 (s, C ortho), 131.3 (s, C para), 123.3 (s, C meta), 72.1 (br s, CH₃O), 63.0 (br s, OCH₂), 28.1 (s, CH(CH₃)₂), 25.4 (s, CH(CH₃)₂). Anal. Calcd for C₁₆H₂₇NCl₃O₂V: C, 45.4; H, 6.4; N, 3.3. Found: C, 44.9; H, 6.2; N, 3.1.

(26) Kaltsoyannis, N.; Mountford, Ph. *J. Chem. Soc., Dalton Trans.* **1999**, 781.

(27) Marquez, A.; Sanz, J. F. *J. Am. Chem. Soc.* **1992**, *114*, 2903.

Synthesis of V(N-2,6-ⁱPr₂C₆H₃)Cl₃(P-P) (P-P = **depe**, **2a**; **dppe**, **2b**). To a solution of V(N-2,6-ⁱPr₂C₆H₃)Cl₃(dme) (**1**) (0.4 g, 0.95 mmol) in THF (30 mL) was added **depe** (0.95 mmol, 0.35 M solution in THF). The mixture was stirred at room temperature for 2 h. The volatiles were removed, and the residue was extracted with dme. Cooling to -20 °C gave orange reddish crystals of **2a** (16% yield). ¹H NMR (300 MHz, C₆D₆): δ 6.95 (d, ³J_{HH} = 7.6 Hz, 2, CH meta), 6.73 (t, ³J_{HH} = 7.6 Hz, 1, CH para), 5.15 (sept, ³J_{HH} = 6.7 Hz, 2, CH(CH₃)₂), 1.45 (d, ³J_{HH} = 6.6 Hz, 12, CH(CH₃)₂), 1.09, 0.76 (dt, J_{HP} = 14.7 Hz, ³J_{HH} = 7.5 Hz, 6, PCH₂CH₃), 2.09 (m, 2, CH₂P), 1.79 (m, 6, CH₂P), 1.40–1.26 (m, 4, CH₂P, obscured by Me resonances). ³¹P{¹H} NMR (C₆D₆): AX spin system, δ 48.3 (br), 14.4 (br). ¹³C{¹H} NMR (75 MHz, C₆D₆): δ 159.0 (s, C ipso), 154.8 (s, C ortho), 129.4 (s, C para), 122.9 (s, C meta), 28.5 (s, CH(CH₃)₂), 25.2 (s, CH(CH₃)₂), 21.7 (dd, J_{CP} = 23.4 Hz, J_{CP} = 16.1 Hz, PCH₂CH₂P), 19.1 (dd, J_{CP} = 10.3 Hz, J_{CP} = 9.2 Hz, PCH₂CH₂P), 18.3 (d, J_{CP} = 19.4 Hz, PCH₂CH₃), 14.1 (d, J_{CP} = 8.9 Hz, PCH₂CH₃), 7.8, 7.6 (d, J_{CP} = 4.1 Hz, PCH₂CH₃). Anal. Calcd for C₂₂H₄₁Cl₃NP₂V: C, 49.0; H, 7.6; N, 2.6. Found: C, 48.8; H, 7.3; N, 2.7.

During the crystallization of **2a** a blue solid precipitated from the mother liquors. Recrystallization from dme gave blue crystals of VOCl₂(**depe**). IR (Nujol): 958 cm⁻¹, ν(V=O). Anal. Calcd for C₁₀H₂₄Cl₂OP₂V·dme: C, 45.2; H, 9.1. Found: C, 45.1; H, 9.1.

To a solution of **1** (0.39 g, 0.92 mmol) in THF (15 mL) was added a solution of **dppe** (0.37 g, 0.92 mmol) in THF (15 mL). The mixture was stirred at room temperature for 2 min, and the volatiles were removed. The residue was washed several times with Et₂O and dried under vacuum. Crude **2b** was obtained in 70% yield. ¹H NMR (300 MHz, C₆D₆): δ 8.05, 7.49, 6.95 (s, Ph, **dppe**), 6.77 (t, ³J_{HH} = 7 Hz, 1, CH para), 5.02 (sept, ³J_{HH} = 6.3 Hz, 2, CH(CH₃)₂), 2.62 (br s, 4, CH₂P), 1.30 (d, ³J_{HH} = 6.3 Hz, 12, CH(CH₃)₂). ³¹P{¹H} NMR (C₆D₆): AX spin system, δ 31.9 (br), -1.5 (br). ¹³C{¹H} NMR (75 MHz, C₆D₆): δ 161.05 (s, C ipso, N-2,6-ⁱPr₂C₆H₃), 156.2 (s, C ortho, N-2,6-ⁱPr₂C₆H₃), 142.1–124.1 (several s, Ph, **dppe**), 129.4 (s, C para, N-2,6-ⁱPr₂C₆H₃), 122.85 (s, C meta, N-2,6-ⁱPr₂C₆H₃), 28.75 (s, CH(CH₃)₂), 24.8 (s, CH(CH₃)₂), 20.2 (br, PCH₂CH₂P). Anal. Calcd for C₃₈H₄₃NCl₃P₂V: C, 62.2; H, 5.9; N, 1.9. Found: C, 60.7; H, 5.6; N, 1.6. No satisfactory analytical data (C percentage) were obtained for this compound.

Computational Details. The electronic structure and geometries of these models were computed within the density functional theory using gradient corrected functionals. In particular, we employed the Becke exchange²⁸ with the Perdew–Wang correlation functional.²⁹ The effective core potential (ECP) approximation of Stevens et al. was used.^{30,31} For V atom, the electrons described by the ECP were those

Table 3. Crystallographic Data for **2a**

| | |
|---|---|
| formula | C ₂₂ H ₄₁ Cl ₃ NP ₂ V |
| fw | 716.14 |
| cryst syst | monoclinic |
| space group | P2 ₁ /c |
| a (Å) | 14.7387(14) |
| b (Å) | 10.6738(10) |
| c (Å) | 16.999(3) |
| β (deg) | 90.954(2) |
| V (Å ³) | 2673.8(6) |
| Z | 4 |
| D _{calc} (g cm ⁻³) | 1.338 |
| μ (mm ⁻¹) | 0.801 |
| T, K | 153(2) |
| λ (Å) | 0.710 73 |
| Θ range (deg) | 2.65–22.99 |
| R ^a | 0.0544 |
| R _w ^b | 0.1046 |

$$^a R = \sum ||F_o| - |F_c|| / \sum |F_o|. \quad ^b R_w = [\sum w(|F_o| - |F_c|)^2 / \sum w|F_o|^2]^{1/2}.$$

of 1s, 2s, and 2p shells, while for 3s, 3p, and valence electrons a basis set of sp type was used with the contraction (8s8p6d)/[4s4p3d]. For P, Cl, N, and C two different approaches were used. In the first, inner electrons were also described through an ECP, and valence electrons were accounted for using a (4s4p)/[2s2p] basis set enlarged with d polarization functions (basis I). In a second series of calculations intended to test the stability of the results against the basis set, these atoms were treated using the all-electron 6-311G(d) basis set (basis II). For H atoms, the standard (4s)/[2s] DZ basis set was used. All of the calculations were performed using the Gaussian-94 package.³²

X-ray Diffraction Study of Complex 2a. A summary of the fundamental crystal data is given in Table 3. A red crystal showing well-defined faces was mounted on a Bruker-Siemens Smart CCD diffractometer equipped with a low-temperature device and normal focus, 2.4 kW sealed tube X-ray source (Mo Kα radiation) operating at 50 kV and 20 mA. Data were collected over a quadrant of the reciprocal space by a combination of two exposure sets. Each exposure of 10 s covered 0.3° in ω. The unit cell dimensions were determined by a least squares refinement using 121 reflections with I > 20σ and 6° < 2θ < 46°. The crystal to detector distance was 6.05 cm. Coverage of the unique set was over 92% complete to at least 23° in θ. The first 50 frames were recollected at the end of the data collection to monitor crystal decay. The intensities were corrected for Lorentz and polarization effects. Scattering factors for neutral atoms and anomalous dispersion corrections for V, Cl, and P were taken from the *International Tables for X-Ray Crystallography*.³³ The structure was solved by Multan and Fourier methods. Full matrix least-squares refinement was carried out by minimizing w(F_o² - F_c²)². H atoms were included in their calculated positions. Refinement was on F² for all reflections. Weighted R factors (R_w) and all goodness of fit S are based on F², and conventional R factors (R) are based on F. Most of the calculations were carried out with SMART³⁴ software for data collection and for data reduction, and SHELXTL³⁴ for structure solution and refinements.

Acknowledgment. This work was supported by the DGES (PB97-740 and PB98-1125) and Junta de Andalucía. We thank Prof. Ernesto Carmona for valuable discussions.

Supporting Information Available: An X-ray crystallographic file in CIF format for the structure determination of complex **1**. This material is available free of charge via the Internet at <http://pubs.acs.org>.

IC9900152

(28) Becke, A. D. *Phys. Rev. A* **1988**, *38*, 3098.

(29) Perdew, J. P.; Wang, Y. *Phys. Rev. B* **1992**, *45*, 13244.

(30) Stevens, W. J.; Basch, H.; Krauss, M. J. *J. Chem. Phys.* **1984**, *81*, 6026.

(31) Stevens, W. J.; Krauss, M.; Basch, H.; Jasien, P. G. *Can. J. Chem.* **1992**, *70*, 612.

(32) Frisch, M. J.; Trucks, G. W.; Schlegel, H. B.; Gill, P. M. W.; Johnson, B. G.; Robb, M. A.; Cheeseman, J. R.; Keith, T.; Petersson, G. A.; Montgomery, J. A.; Raghavachari, K.; Al-Laham, M. A.; Zakrzewski, V. G.; Ortiz, J. V.; Foresman, J. B.; Cioslowski, J.; Stefanow, B. B.; Nanayakkara, A.; Challacombe, M.; Peng, C. Y.; Ayala, P. Y.; Chen, W.; Wong, M. W.; Andres, J. L.; Replogle, E. S.; Gomperts, R.; Martin, R. L.; Fox, D. J.; Binkley, J. S.; Defrees, D. J.; Baker, J.; Stewart, J. P.; Head-Gordon, M.; González, C.; Pople, J. A. *Gaussian 94*, Revision D.2; Gaussian, Inc.: Pittsburgh, PA, 1995.

(33) *International Tables for X-Ray Crystallography*; Kynoch Press: Birmingham, U.K., 1974; Vol. 4, pp 72–98.

(34) SHELXTL, Siemens Energy & Automation Inc., Analytical Instrumentation, 1996.